5

ALK1Fc suppresses tumor growth by impairing angiogenesis and proliferation of human prostate cancer cells *in vivo*

Eugenio Zoni*
Sofia Karkampouna*
Peter C. Gray
Marie-José Goumans
Lukas J.A.C. Hawinkels
Gabri van der Pluijm
Peter ten Dijke
Marianna Kruithof-de Julio

*Authors Contributed Equally

Adapted from Manuscript Submitted

Abstract

Prostate cancer is the second most common cancer in men worldwide. Despite current therapies, when cancer progress, patient develop metastasis, mainly in the bones. Therefore, targeting the molecular pathways that underlie primary tumor growth and spread of metastases is of great clinical value. Bone morphogenetic proteins (BMPs) play a critical role in prostate cancer. BMP9 and the closely related BMP10 signal via the transmembrane serine kinase receptors *A*ctivin receptor-*L*ike *K*inase 1 (ALK1) and ALK2 and the cytoplasmic proteins SMAD1 and SMAD5. The human ALK1 extracellular domain (ECD) binds BMP9 and BMP10 with high affinity and we show that a soluble chimeric protein consisting of the ALK1 ECD fused to human Fc (ALK1Fc) prevents activation of endogenous signaling via ALK1 and ALK2. We also show for the first time in prostate cancer that ALK1Fc reduces BMP9-mediated signaling and decreases tumor cell proliferation *in vitro.* In line with these observations, we demonstrate that ALK1Fc impairs angiogenesis and reduces tumor growth *in vivo.* Our data show that BMP9 correlates with poor survival and is upregulated in high risk prostate cancer patients. We identify BMP9 as a putative therapeutic target and ALK1Fc as a potential therapy capable of targeting tumor cells and the supportive tumor angiogenesis. Together these findings justify the continued clinical development of drugs blocking ALK1 and ALK2 receptor activity.

Introduction

Prostate cancer is the second most common cancer in men worldwide (1). Currently prostate cancer, when still in its first phase of androgen dependency, can be successfully treated surgically. However, once the cancer develops in an androgen-independent state, therapy is no longer useful or successful and lethality is almost invariably due to the consequences of metastasis. Therefore, understanding the molecular pathways that underlie the emergence and spread of metastases from primary tumors are of great biological and clinical value.

Expression of several BMPs has been examined in prostatic tissue with benign prostatic hyperplasia (BPH), non-metastatic and metastatic prostatic adenocarcinoma and has been associated with cancer aggressiveness (2). However, little is known about the roles of BMP9 and BMP10 and their signaling receptors, ALK1 and ALK2, in prostate cancer and particularly in androgen independent and metastatic prostate cancer. Previous studies have highlighted the role of ALK1 as key regulator of normal as well as tumor angiogenesis (3, 4). BMP9 and BMP10 are high affinity ligands for ALK1, which is predominantly expressed in endothelial cells (5). Alternatively, BMP9 signals through the BMP type I receptor ALK2 (6-8). Binding of BMP9/BMP10 to ALK1/ALK2 results in phosphorylation and activation of downstream effectors SMAD1/SMAD4 and/or SMAD5 (7-9). In ovarian cancer, BMP9 acts as proliferative factor, promoting human epithelial ovarian cancer and human immortalized ovarian surface epithelial cell proliferation through ALK2/SMAD1/SMAD4 pathway (8). Similarly, BMP9 stimulates proliferation of liver cancer cells (10) and osteosarcoma growth (11). Among the BMPs, BMP9 is the most recently identified (12) and least studied ligand. Current research has not only attributed a tumor-promoting role to BMP9 (8, 10, 11) but also tumor suppressing properties (13-15) in different types of cancer, including prostate cancer.

Several studies have highlighted the role of BMP9/ALK1 in the genetics and development of blood vessel formation, outlining its critical involvement in pathological and tumor angiogenesis (16, 17). Interestingly, alterations of signal transduction pathways that are important for blood vessel formation, such as the NOTCH pathway, have also been associated with arterio-venous malformations (18, 19). Recently, BMP9 and BMP10 signaling were linked to NOTCH signaling, one of the major pathways involved in prostate cancer development, progression and bone metastasis (20). Expression profiling studies have shown that members of the NOTCH pathway are characteristic of high grade (Gleason 4+4=8) micro-dissected prostate cancer cells compared to low grade (Gleason 3+3=6) (21). Moreover, inhibition of NOTCH1 reduces prostate cancer cell growth, migration and invasion (22). Interestingly, NOTCH signaling pathway activates ALDH1A1, a well-known marker of prostate cancer stem cells (23-26).

In order to understand the role of BMP9 in prostate cancer tumor progression, we employed the soluble chimeric protein ALK1Fc (ACE-041) (27) which binds BMP9 and BMP10 with high affinity and blocks their signaling via ALK1 and ALK2 receptors by acting as a ligand trap (28, 29). BMP9 induces endothelial cell proliferation and vessel formation (30) while ALK1Fc has previously been shown to inhibit vascularization and tumor growth of breast cancer *in vivo* in an orthotopic transplantation model (28). ALK1Fc binds and neutralizes only BMP9 and BMP10 ligands and not TGFβ (28, 29), which also plays important roles in angiogenic processes. Phase I clinical trials have been completed using ALK1Fc as anti-angiogenesis therapy in myeloma (clinicaltrials.gov identifier NCT00996957).

Here we show, for the first time in prostate cancer, that ALK1Fc reduces BMP9 signaling and decreases proliferation of highly metastatic and tumor initiating human prostate cancer cells *in vitro.* We further demonstrate that ALK1Fc impairs angiogenesis, affects tumor cell proliferation and reduces tumor growth *in vivo.* Taken together these data suggest BMP9 as a possible therapeutic target in prostate cancer and justify the continued clinical development of additional drugs that block signaling via ALK1 and ALK2.

Materials and Methods

Cell line and culture conditions

The human osteotropic prostate cancer cell line PC-3M-Pro4luc2 (31) was maintained in DMEM supplemented with 10% FCII, 0.8 mg/ml Neomycin (Santacruz, Dallas, USA) and 1% Penicillin-Streptomycin (Life Technologies, Carlsbad, USA). C4-2B cells were maintained in T-medium DMEM (Sigma-Aldrich, The Netherlands) supplemented with 20% F-12K nutrient mixture Kaighn's modification (GibcoBRL), 10% FCS, 0.125 mg/ml biotin, 1% Insulin-Transferin-Selenium, 6.825 ng/ml T3, 12.5 mg/ml adenine and 1% penicillin/streptomycin. Cells were maintained at 37°C with 5% CO_2.

Luciferase reporter gene constructs

PC-3M-Pro4Luc2 cells were seeded at a density of 50,000 cells in 500 µL medium in a 24-well plate. Transient transfection of reporter constructs was performed with Lipofectamine2000 (Life Technologies) according manufacturer's protocol. For each well, 100 ng of NICD-*ff-luciferase*,10 ng CAGGS-*Renilla luciferase,* 100 ng BRE renilla and 100 ng BREluc/well were transfected. After 24 hours, medium was replaced and cells were treated with BMP9 for 24h. The *Firefly* luciferase and *Renilla* luciferase levels in the lysates were measured using Dual Luciferase Assay (Promega, Madison, USA).

RNA isolation and real-time qPCR

Total RNA was isolated with Trizol Reagent (Invitrogen, Waltham, USA) and cDNA was synthesized by reverse transcription (Promega, Madison, USA) according to the manufacturer's protocol. qRT-PCR was performed with Biorad CFX96 system (Biorad, Veenendaal, The Netherlands). Gene expression was normalized to GAPDH or β-actin. (For primer sequences see Supplementary Table I). Total RNA from frozen section (5µm) was isolated with Qiagen Mini Isolation kit (Venlo, The Netherlands) according to the manufacturer's protocol. Primer sequences are listed in Suppl. Table 1.

MTS assay

Cells were seeded at density of 2,000 cells/well and treated with ALK1Fc or CFc (10ug/ml, Acceleron, USA) allowed to grow for 24, 48, 72 and 96 hours. After incubation, 20 µl of 3-(4,5 dimethylthiazol- 2- yl)- 5 -(3 -carboxymethoxyphenyl)- 2 -(4 -sulfophenyl)- 2 H-tetrazolium was added and mitochondrial activity was measured after 2 hours incubation at 37°C. MTS absorbance values are positively proportional to total number of metabolically active cells providing an indirect correlation with cell proliferation rate (50) (CellTiter96 Aqueous Non-radioactive Cell proliferation assay, Promega).

Animals

Male 6-8 week-old athymic nude mice (Balb/c *nu/nu*), purchased from Charles River (L'Arbresle, France), were used in all *in vivo* experiments (n=15 per group). Mice were housed in individual ventilated cages under sterile condition, and sterile food and water were provided *ad libitum*. Animal experiments were approved by the local committee for animal health ethics and research of Leiden University (DEC #11246), and carried out in accordance with European Communities Council Directive 86/609/EEC. After the experimental periods, mice were injected with hypoxia probe (6mg/kg, Burlington, Massachusetts, USA) and lectin-Tomato (1 mg/kg, Vector Laboratories, USA) intravenously prior to perfusion and sacrified according to our mouse protocol. Tumors were dissected and processed for further histomorphological analysis as described below.

Orthotopic prostate transplantation and ALK1Fc treatment

25000 PC-3M-Pro4luc2 cells (10 ul final volume) were injected in the dorsal lobe of nude mice. In brief: After anesthetizing the mice with isoflurane, each mouse was placed on its back and a small incision was made along the lower midline of the peritoneum for about 1 cm. The prostate dorsal lobes were exteriorized and stabilized gently. A 30-gauge needle attached to a 1-cc syringe was inserted into the right dorsal lobe of the prostate. 10 µl of the material was slowly injected. A well-localized bleb indicates a successful injection. After retracting the needle a Q-tip was placed over the injection site for about 1 min to prevent bleeding and spillage of material. The prostate was then returned to the peritoneum and the abdominal wall and skin layer was sutured. After establishment of the primary tumor, at 10 days after the orthotopic transplantation, mice were intraperitoneally injected with Control-Fc (CFc) or ALK1Fc compounds (1 mg/kg) twice per week. Administration of compounds was performed for four weeks. ALK1-Fc is a fusion protein comprised of the extracellular domain of human ALK1 fused to the Fc region of IgG and was obtained from Acceleron Pharma, Cambridge, USA. The Fc domain of IgG_1 was used as a control (MOPC-21; Bio Express, West Lebanon NH).

Whole body bioluminescent imaging (BLI)

Tumor growth was monitored weekly by whole body bioluminescent imaging (BLI) using an intensified-charge-coupled device (I-CCD) video camera of the *in vivo* Imaging System (IVIS100, Xenogen/Perkin Elmer, Alameda, CA, USA) as described previously (51). In the SD-208 in vivo treatment experiment the newer IVIS Lumina II (Xenogen/Perkin Elmer, Alameda, CA, USA) was used for BLI measurements. Mice were anesthetized using isoflurane and injected intraperitoneally with 2 mg D-luciferin (Per bio Science Nederland B.V., Etten-Leur, the Netherlands). Analyses for each tumors were

performed after definition of the region of interest and quantified with Living Image 4.2 (Caliper Life Sciences, Teralfene, Belgium). Values are expressed as relative light units (RLU) in photons/sec.

Immunofluorescence

Immunofluorescence staining was performed as described previously (52). In brief, Immunofluorescence staining was performed on 5-µm paraffin embedded sections. For antigen retrieval, sections were boiled in antigen unmasking solution (Vector Labs, Peterborough, UK) and stained with CD31 (Sigma) or ALDH1A1 (Abcam) antibodies. Sections were blocked with 1% bovine serum albumin (BSA)-PBS-0.1% v/v Tween-20 and incubated with primary antibodies diluted in the blocking solution, overnight at 4°C or room temperature. Sections then were incubated with secondary antibodies labelled with Alexa Fluor 488, 555, or 647 (Invitrogen/Molecular Probes, Waltham, USA) at 1:250 in PBS-0.1% Tween-20. Nuclei were visualized by TO-PRO3 (Invitrogen/Molecular Probes, 1:1000 diluted in PBS-0.1% Tween-20) or DAPI, which was included in the mounting medium (Prolong G, Invitrogen/Molecular Probes).

Western immunoblotting

Proteins were extracted by using RIPA buffer (Thermo Scientific) and protein concentrations were quantified according to manufacturer's protocol (Thermo Scientific). Proteins samples (20 µg per sample) were separated by 15% SDS-PAGE followed by transfer to a blotting membrane. The membrane was blocked with 5% Milk, dissolved in PBS-Tween for 1 hour at room temperature. The membrane was incubated with 1:1000 primary antibody (anti-NOTCH1, Cell Signaling, catalogue number 3608) at 4ºC overnight. Subsequently, the membrane was incubated with 1:10000 secondary horseradish peroxidase (HRP) antibody. All antibodies were dissolved in PBS-Tween. Chemi-luminescence was used to visualize the bands.

Clonogenic assay

Clonogenic assay was performed in 6 well plate. 100 cells were seeded in 2mL of medium and incubated at 37°C in presence of 5% CO_2 for two weeks. Plates were washed with PBS and cells fixed for 5 min with a solution of 4% PFA. Colonies were stained with 0.1% crystal violet (Sigma-Aldrich, The Netherlands) and plates were imaged before processing the data (53).

Statistical analysis

Statistical analysis was performed with GraphPad Prism 6.0 (GraphPad software) using t-test or ANOVA for comparison between more groups. Data is presented as mean ± SEM. P-values ≤ 0.05 were considered to be statistically significant (* $P < 0.05$, ** $P < 0.01$, *** $P < 0.001$).

Results

High expression of BMP9 and ALK1 correlates with poor survival

We investigated the correlation of survival with BMP9 and ALK1 expression in an independent publically available PCa dataset (GSE21032). BMP9 and ALK1 expression were associated with poor prognosis (**Fig. 1 A and B top**; Hazard Ratio (HR)=2.38 and p=0.007 for BMP9 and HR=2.62 and p=0.007 for ALK1). Additionally, the expression of BMP9 and ALK1 in stratified risk groups was significantly higher in the high vs. low risk group (**Fig. 1 A and B Bottom**; p=1.3e-34 for BMP9 and p=3.46e-19 for ALK1). Taken together, these data demonstrate that BMP9 and ALK1 are selectively highly expressed in aggressive PCa and that their expression correlates with poor prognosis.

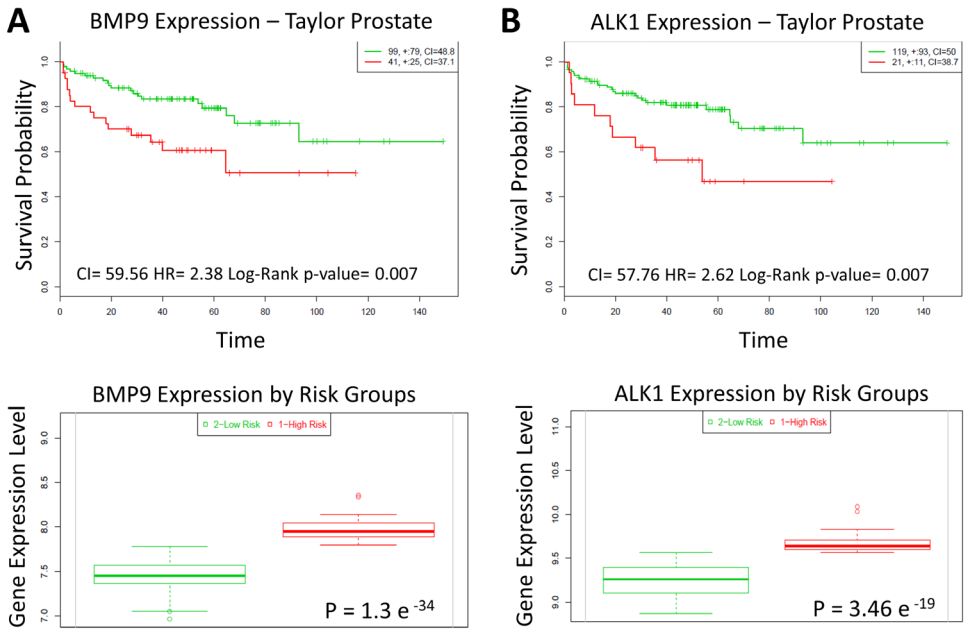

Figure 1. BMP9 and ALK1 correlate with poor patient prognosis. A-B) Top panels: Kaplan-Meier survival curves of censored Cox analysis in Taylor-MSKCC prostate database stratified by maximized BMP9 and ALK1 expression risk groups. Red = high expression; Green = low expression. Bottom panels: BMP9 and ALK1 expression levels stratified by risk groups. Red = high Risk and high BMP9 and ALK1 expression; Green = low risk and low BMP9 and ALK1 expression.

ALK1Fc reduces primary prostate tumor burden *in vivo*

To investigate the role of BMP9 in prostate cancer progression, ALK1Fc was administered in a mouse model of prostate cancer. Orthotopic prostate tumor growth was induced by intra-prostatic inoculation of human prostate cancer PC-3M-Pro4luc2 cells in Balb/c nude mice and tumor progression was followed by bioluminescence imaging (BLI) (31) (**Fig.2A**). Based on the BLI signal the mice were distributed between two treatment groups: ALK1Fc or CFc (n=15 per group). The compounds were injected twice weekly and tumor imaging and body weights were monitored weekly for 5 weeks (**Suppl. Fig.1**). Tumor burden was quantitatively assessed for each animal during the course of treatment. The group of animals that received ALK1Fc exhibit smaller tumor size compared to the animals that received CFc based on the size after resection (**Fig. 2B**) and bioluminescence quantification (**Fig. 2C**, p<0.001).

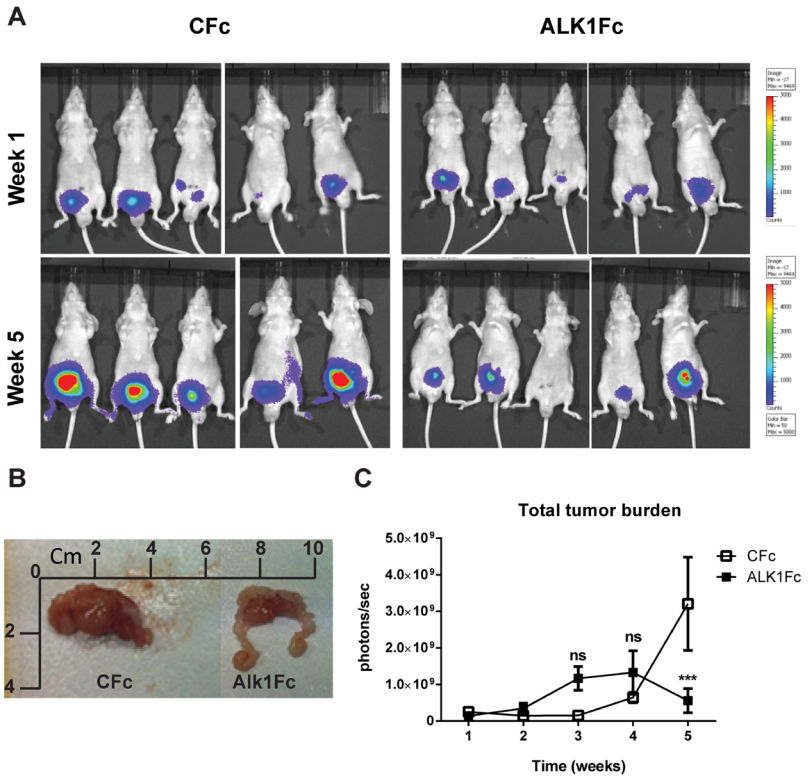

Figure 2. Effect of ALK1Fc *in vivo*. A) PC-3M-Pro4Luc2 cells were orthotopically injected in the anterior lobe of prostate glands of nude mice (n=15 per group). Detection of primary tumor burden was observed at 2 weeks after injection, with the time point designated as "week 1" at the start of treatment with ALK1Fc or CFc. Representative examples of bioluminescent images of tumor burden at the start of treatment with ALK1Fc/ CFc (week 1) and at the end point (week 5). **B**) Representative images of primary

tumor size (in centimeters) from a recipient of CFc versus ALK1Fc treatment after 5 weeks. **C**) Quantification of bioluminescent signal (photons/sec) in mice treated with either CFc (n=14) or ALK1Fc (n=15) for 5 weeks. Error bars indicate ± SEM. P value <0.001 (***).

Alk1Fc reduces vascular density of the primary prostate tumor

The degree of tumor angiogenesis is critical for progressive tumor growth beyond a few mm^3 in size. Intravenous lectin perfusion was used to map the perfused elements of the tumor vasculature in mice. Fluorescent-conjugated lectin (lectin-Tomato) was visualized in tumor tissue sections and quantified. Vascular density, indicated by the overall lectin presence, was decreased in the tumors treated with ALK1Fc compared to the CFc group (**Fig. 3A, B**). We evaluated the presence of endothelial cells in tumor sections by CD31 immunofluorescence. CD31 expression was decreased after treatment with ALK1Fc indicating fewer endothelial cells and vessels (**Fig. 3C, D**). Hypoxia is an important component of angiogenesis and critical for tumor formation. A hypoxia-induced probe was injected in tumor bearing mice just prior to sacrifice and the hypoxic areas within the tumors were visualized after tumor resection (**Fig. 3E, F**). Hypoxic areas are found in both treatment groups; however, the overall amount of hypoxia is significantly higher ($p< 0.05$) in ALK1Fc-treated, tumor-bearing mice over the CFc-treated groups. We assessed the presence of cell proliferation and cell death in these tumors by immunofluorescence for the mitosis marker phosphorylated histone 3 (PH3) and the apoptosis marker cleaved caspase 3 (CASP3). Dividing PH3 positive cells are predominantly located in normoxic areas (**Fig.3E, left panel**). Quantification of immunofluorescence signal shows that the number of dividing cells is lower in the ALK1Fc-treated animals (**Fig. 3G**; $p<0.05$). Detection of apoptotic cells (Caspase-3 positive) is higher in the ALK1Fc-treated tumors (**Fig. 3H**; $p<0.05$) and occurs mostly, however not exclusively, in hypoxic areas (**Fig.3E**), suggesting a correlation between the hypoxia and tumor cell death.

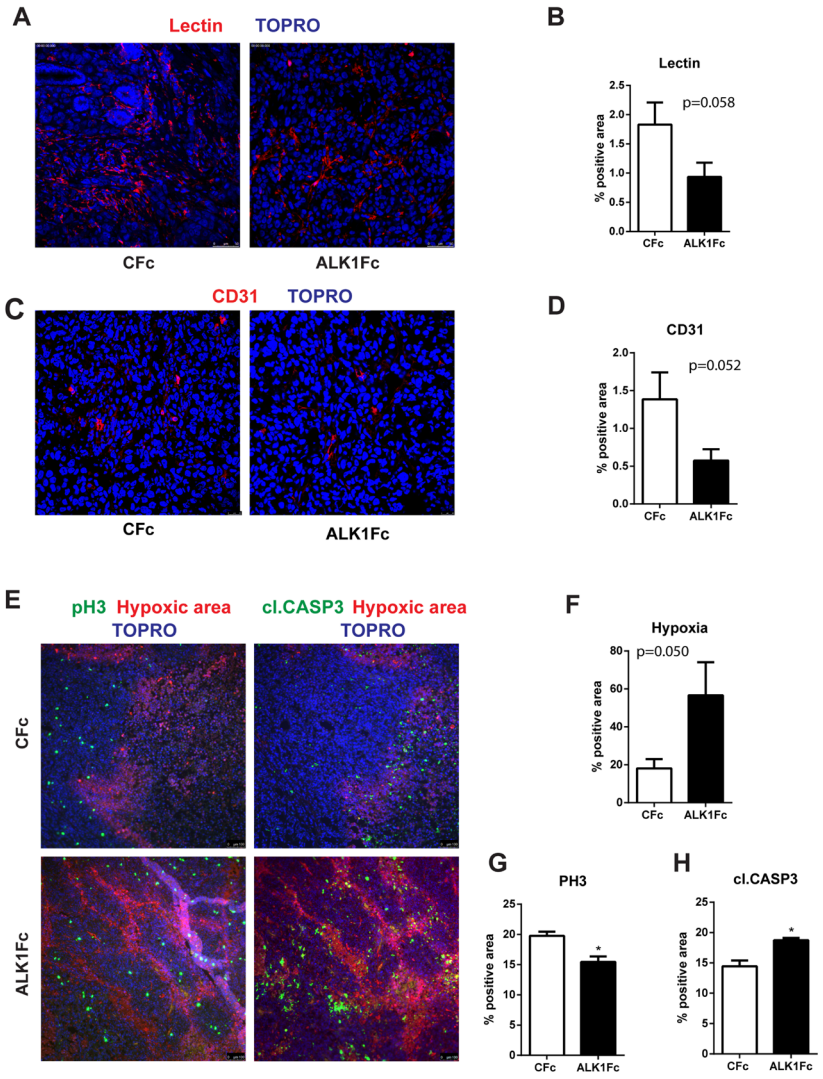

Figure 3. Effect of ALK1Fc on vascular density, cell proliferation and apoptosis *in vivo*. **A**) Representative images of lectin detection in primary prostate tumor samples after perfusion with fluorescent-labelled lectin-Tomato (red). TOPRO (blue) marks the nuclei. Treatment groups: ALK1Fc or CFc. **B**) Quantification of lectin positive surface area in all tumor samples of each group (n=6 for CFc, n=7 for ALK1Fc). (**C**) Representative images of CD31 (red) immunofluorescence staining in primary prostate tumor samples after 5 weeks of treatment with either ALK1Fc or CFc. **D**) Quantification of CD31 positive surface area in all tumor samples of each group (n=6 for CFc, n=7 for ALK1Fc). **E**) Representative images of hypoxia immunofluorescence staining (red) in primary prostate tumor samples after 5 weeks of treatment with either ALK1Fc or CFc. Hypoxia probe was injected prior to sacrifice and was detected by a specific fluorescent antibody. Immunofluorescence images for colocalization of apoptotic or proliferating cells in hypoxic/ normoxic area within the prostate tumor area in ALK1Fc and CFc treated

animals. pH3: PhosphoHistone 3 proliferation marker (green); cleaved caspase 3 apoptosis marker (green); Hypoxic probe-antibody; hypoxic area (red). **F**) Quantification of hypoxia positive area in all tumor samples of each group (n=6 for CFc, n=7 for ALK1Fc). **G**) Quantification of pH3 positive area in all tumor samples of each group (n=6 for CFc, n=7 for ALK1Fc). **H**) Quantification of cleaved caspase 3 positive (apoptotic cells) in all tumor samples of each group (n=6 for CFc, n=7 for ALK1Fc).

ALK1Fc decreases proliferation of human prostate cancer cells

To investigate how ALK1Fc can decrease tumor growth, we investigated the effect of ALK1Fc on prostate cancer cells. We measured the mRNA levels of BMP9 type I receptors ALK1 and ALK2 in the PC-3M-Pro4Luc2 (31) human prostate cancer cell line and tested the response of these cells to BMP9. Consistent with what was previously reported in highly metastatic PC-3 and PC-3M prostate cancer cells (32), qRT-PCR analysis in osteotropic PC-3M-Pro4Luc2 cells revealed undetectable levels of ALK1 mRNA but clearly measurable levels of ALK2 mRNA (**Suppl. Fig. 2A**). Treatment with BMP9 showed a dose-dependent induction of BRE-*Renilla* luciferase activity in PC-3M-Pro4Luc2 cells (p-value=0.005 and 0.05 with 0.5 nM and 1 nM BMP9, respectively) indicative of conserved and active signaling machinery (**Suppl. Fig. 2B**). Using the 1nM BMP9 dose for subsequent experiments, we tested the combined effect of BMP9 with either ALK1Fc or CFc on BRE reporter assay. Treatment with ALK1Fc (10 ug/mL) completely abolished the BMP9-mediated BRE luciferase (luc) activity (**Suppl. Fig. 2C**; BMP9+ALK1Fc) to levels similar to the non-stimulated control (Untreated). Treatment with BMP9+CFc (10 ug/mL) led to induction of BRE-luc activity of similar level as the BMP9 treatment (**Suppl. Fig. 2C**; p-value <0.05). Taken together, these results indicate that ALK1Fc blocks ALK2-mediated BMP9 signaling in PC-3M-Pro4Luc2 cells.

We further show that treatment of with 10 ug/mL ALK1Fc, but not control Fc (CFc), strongly reduced BMP9-induced PC-3M-Pro4Luc2 cell proliferation (p<0.001 at day 4 comparing vehicle vs BMP9 or ALK1Fc treatment, respectively) (**Fig. 4A**). The effect of ALK1Fc on cell proliferation appeared to be specific since it had no effect on cell proliferation in the absence of BMP9 treatment (**Suppl. Fig.2D**). The proliferative effect of BMP9 was also tested in the C4-2B prostate cancer cell line; however no significant difference was observed (**Suppl. Fig. 2E**). When we treated PC-3M-Pro4Luc2 cells with BMP9 in combination with an ALK2 kinase inhibitor (LDN193189, LDN) (33, 34) we observed a complete loss of BMP9-induced proliferation (**Fig. 4B**). LDN treatment also blocked BMP9 stimulation of the BRE-luc reporter in PC-3M-Pro4 cells (**Suppl. Fig. 2F**) but had minimal impact on basal proliferation levels in the absence of exogenously added BMP9 (**Suppl. Fig. 2G**). Finally, we evaluated the clonogenic ability of PC-3M-Pro4Luc2 cells after BMP9 treatment alone (**Suppl. Fig.3A**) and confirmed that BMP9 affects cell proliferation, strongly increasing the size of the colonies (**Suppl. Fig.3B**,

p<0.05). However, BMP9 showed no effect on colony formation/self-renewal ability of PC-3M-Pro4Luc2 since the total number of colonies formed is similar (**Suppl. Fig. 3C**). Together, these data indicate that ALK1Fc strongly reduces BMP9- induced proliferation of human prostate cancer cells.

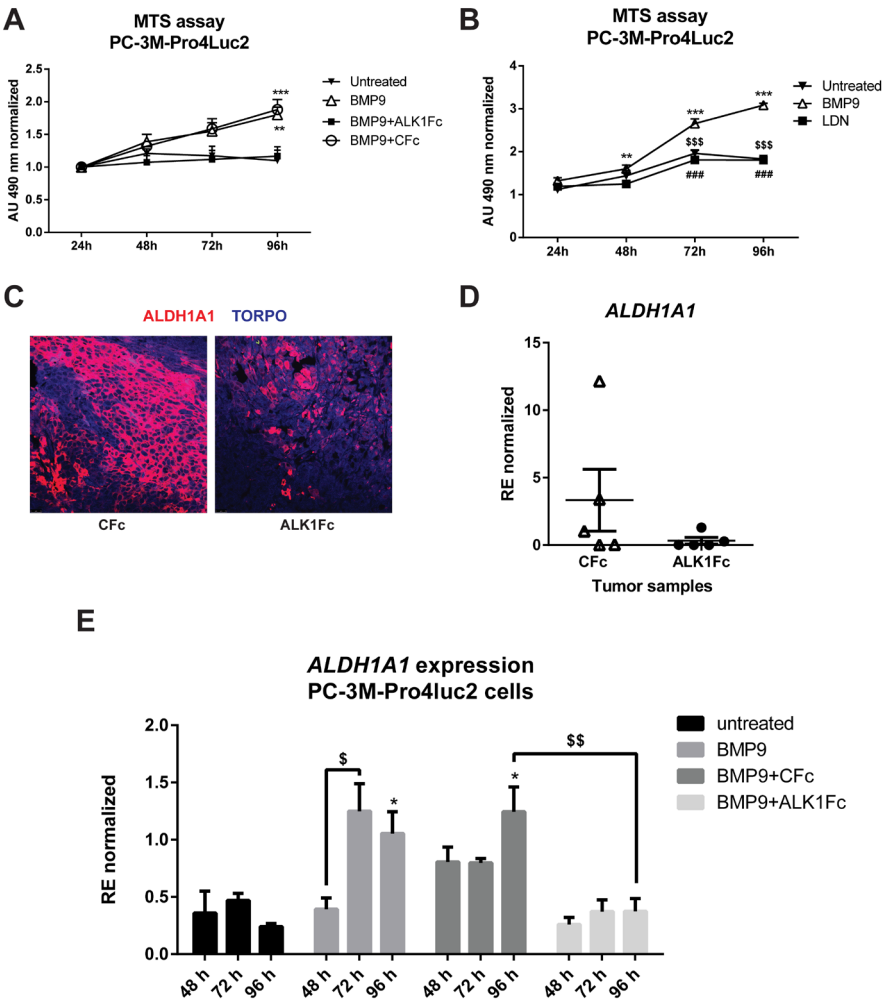

Figure 4. Effect of BMP9 and ALK1Fc on proliferation and ALDH1A1 expression. **A**) MTS assay (24, 48, 72, 96 hours) was performed in PC-3M-Pro4Luc2 cells stimulated with recombinant BMP9 (1 nM), BMP9 (1 nM)+ALK1Fc (10 ug/ml) or BMP9 (1 nM)+CFc (10 ug/ml). Accumulation of MTS was measured based on absorbance at 490 nm. Values are normalized to the basal measurements at 24 hours after cell seeding and treatments. Graph represents values for three independent experiments (n=3). Error bars indicate ± SEM. P value < 0.01 (**) BMP9 vs Untreated and P-value < 0.001 (***) BMP9+CFc vs Untreated. **B**) MTS assay (24, 48, 72 and 96 hours). PC-3M-Pro4Luc2 cells were seeded at low density in 96-well plates and

treated with BMP9 (1 nM), LDN (BMP type I receptor inhibitor LDN193189, 120nM) or LDN+BMP9. (n=2). Error bars indicate SEM. **C**) Representative images of ALDH1A1 immunofluorescence in prostate tumor samples from ALK1Fc and CFc treated animals. ALDH1A1: red; TOPRO: blue nuclear dye. **D**) Quantification of ALDH1A1 mRNA by Q-PCR in tumor samples of each group (n=5 for CFc, n=5 for ALK1Fc). **E**) Expression of ALDH1A1 in PC-3M-Pro4Luc2 cells. Relative mRNA expression was measured by Q-PCR from cDNA obtained from PC-3M-Pro4Luc2 cells treated with BMP9, BMP9+ALK1Fc, BMP9+CFc, for 48, 72 and 96 hours. Values are normalized to β-actin expression. Error bars are ±SEM (n=3).

Expression of BMP9, ALK1 and ALK2 in human and murine prostate tumor tissues

We investigated the mRNA expression of BMP9, ALK1 and ALK2 in 48 benign prostate tumors and 47 malignant prostate tumors (35) using bioinformatics analysis and data mining platforms (R2: microarray analysis and visualization platform http://r2.amc.nl, source: GEO ID: GSE29079) (**Suppl. Fig.3D, E and F**). While levels of *ALK1* transcripts are decreased in the malignant tumor group compared to the benign group ($p<0.001$), levels of *ALK2* transcripts are significantly increased ($p<0.01$) in the malignant tumor group compared to the benign group. BMP9 mRNA expression is similar in both groups ($p=0.28$). Previously, Bacac *et al.* (36) performed cDNA microarray analysis using laser-micro dissected stromal cells from murine prostate intraepithelial neoplasia (PIN) and invasive prostate tumors. Analysis of *ALK1, ALK2* and *BMP9* (**Suppl. Fig.3G, H and I**) expression in this dataset indicated elevated mRNA expression of *ALK1*, *ALK2* and *BMP9* during the invasive stage of murine prostate cancer.

ALK1Fc inhibits ALDH1A1 expression *in vivo* and interferes with NOTCH signaling

Given its ability to reduce primary tumor burden and block BMP9-induced tumor cell proliferation *in vitro* we assessed the effects of ALK1Fc on the relative expression of the *ALDH1A1* marker that is associated with cancer stem cell-like cells and poor patient prognosis (25, 26). Treatment of prostate tumor bearing mice with ALK1Fc affected the number of proliferative ALDH1A1 positive cells in the prostate tumor tissues both at protein (**Fig. 4C**) and mRNA level (**Fig. 4D**). *In vitro* stimulation with BMP9 of the same cell line used to induce tumors in the xenograft mouse model, confirmed that treatment with BMP9 or BMP9+CFc upregulates ALDH1A1 expression while BMP9+ALK1Fc treatments does not have any effect (**Fig. 4E**).

ALDH1A1 is known to be regulated by NOTCH signaling (23-25) and NOTCH1 plays a prominent role in prostate cancer cell proliferation and migration (22, 37-40). Larrivée et al. have shown that ALK1 and NOTCH converge on common downstream pathways and that BMP9 treatment alone upregulates JAG1 expression in HUVEC non-transformed

cells (41). To verify the effect of BMP9 on NOTCH signaling activation in our cancer model, we used qRT-PCR to quantify the expression of *JAG1* after BMP9 stimulation in presence of ALK1Fc or CFc. Our transcriptional analysis showed that BMP9 and BMP9+CFc induce mRNA expression of *JAG1* and that ALK1Fc reduces the BMP9-mediated induction of *JAG1* (**Fig. 5A**). To assess the clinical relevance of BMP9/ALK2-mediated NOTCH pathway activation in human prostate cancer, we performed bioinformatics analysis using data mining platforms (R2: microarray analysis and visualization platform http://r2.amc.nl, source: GEO ID: GSE29079). Transcript levels of the NOTCH ligand *JAG1* were significantly higher in the malignant tumor group compared to the benign group (**Fig. 5B**) and positively correlate with *ALK2* expression and disease progression (**Fig.5D**). In addition, the prostate tumor microarray data indicate a positive correlation between the level of *NOTCH1* receptor expression and human progression to malignancy (**Fig. 5C**) as well as *ALK2* expression (**Fig. 5E**). In addition, overexpression of JAG1 in PC-3M-Pro4Luc2 human prostate cancer cells increases metabolic activity measured by MTS assay (**Fig. 5F**).

We targeted expression of NOTCH1 in PC-3M-Pro4Luc2 using a specific shRNA (shNOTCH1) and assessed resulting NOTCH1 levels by western blot and by reporter assay (**Suppl. Fig. 4A and B**). NOTCH1 knockdown cells had decreased proliferation compared to cells transduced with non-targeting shRNA lentivirus ($p<0.05$ at 48h and at 72h) (**Fig. 5G**). We observe that stimulation of shNOTCH1-cells with BMP9 increases their proliferation rate (**Fig. 5H**) and that shNOTCH1-cells display decreased levels of JAG1 mRNA (**Suppl. Fig . 4C**). These data suggest that BMP9/ALK2 induces activation of NOTCH signaling (JAG1 and NOTCH1) and enhanced cell proliferation both of which are associated with tumor progression in PCa.

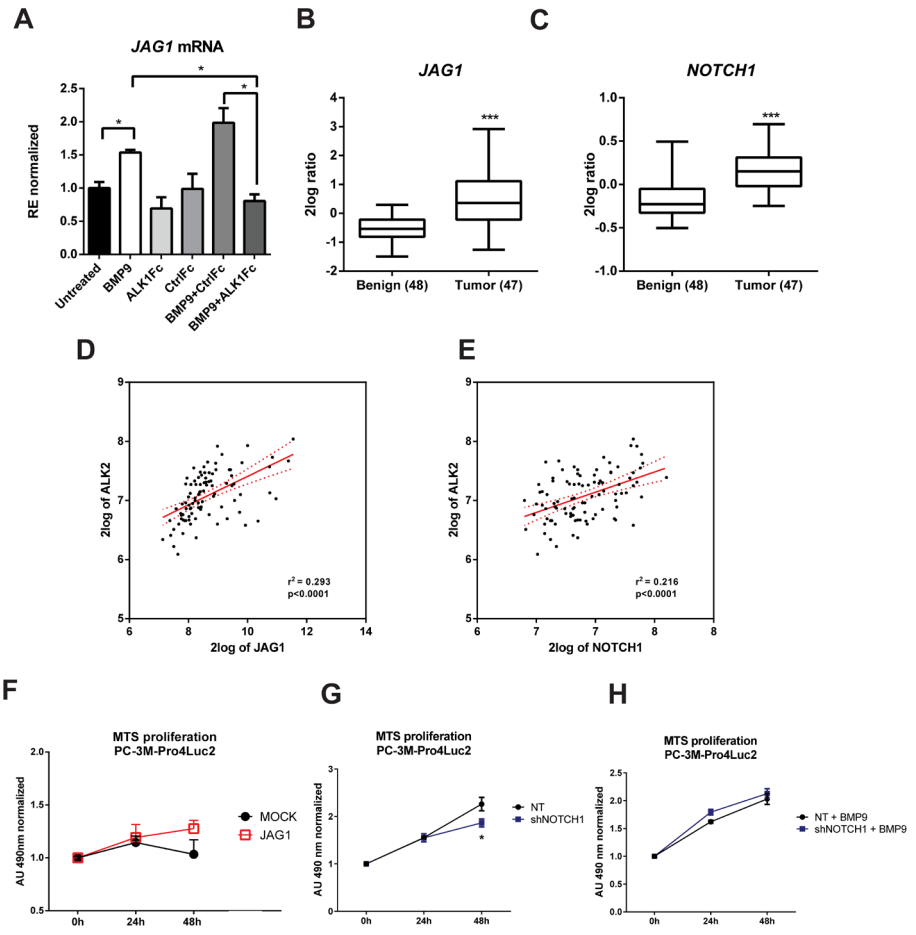

Figure 5. Effect of BMP9 and ALK1Fc on NOTCH signaling pathway and correlation study. A) Expression of *JAG1* in PC-3M-Pro4Luc2 cells. Relative mRNA expression was measured by qPCR from cDNA obtained from PC-3M-Pro4Luc2 cells treated with BMP9, ALK1Fc, CFc, BMP9+ALK1Fc or BMP9+CFc for 96 hours. Values are normalized to β-actin expression. Error bars are ±SEM (n=3). **B-C**) Bioinformatics analysis of AMC OncoGenomics database (Sueltman transcript comparison) showing mRNA expression of *JAG1* **B**) and *NOTCH1* **C**) in prostate tissues among benign prostate tissues (n=48) versus tumor tissues (n=47). Values are expressed as 2log ratio tumor/ benign. ns: not significant. P value < 0.001 (***). **D**) Correlation analysis of *JAG1* and *ALK2* expression (p<0.0001) and **E**) correlation analysis of NOTCH1 and ALK2 expression (p<0.0001) in prostate tissues among benign prostate tissues (n=48) versus tumor tissues (n=47). Bioinformatic analysis was performed using the AMC OncoGenomics database (Sueltman transcript comparison), values are expressed as 2log ratio tumor/ benign. ns: not significant. **F**) MTS assay (24, 48 hours) in PC-3M-Pro4Luc2 cells transfected with 1ug JAG1 or Mock expression vector (n=2). **G-H**) MTS assay (24, 48, 72 and 96 hours) in PC-3M-Pro4Luc2 cells were transduced with short hairpin RNA against NOTCH1 (shNOTCH1) lentiviral vector or non-targeting (NT) shRNA vector (mock) and

plated at low density. Treatment with BMP9 (1 nM) was done once at cell seeding (t=0) MTS absorbance was measured. Values are normalized to the basal measurements t=0 after cell seeding and treatments. Graph represents values for three independent experiments (n=3). Error bars indicate SEM. P value <0.05 (*).

Discussion

In this study, we find that BMP9 and ALK1 correlate with poor survival in prostate cancer patients and that BMP9 has a tumor-promoting effect on human prostate cancer cells both *in vitro* and *in vivo*. We demonstrate that blocking BMP9 signaling with ALK1Fc efficiently diminishes prostate cancer cell proliferation and substantially attenuates tumor growth in an orthotopic model of human prostate cancer.

BMP9 was first identified in the liver (12) and active forms are present in serum (8). BMP9 is a ligand for the ALK1 receptor in endothelial cells (5) and exerts stimulatory or inhibitory effects on endothelial cell growth and migration depending on the cellular context (30, 42). Aberrant regulation of TGF-β and BMP signaling often results in cancer progression (43, 44). In particular, BMP ligands, such as BMP9 as well as BMP type I receptors (e.g. ALK1 and ALK2) have been associated with tumor angiogenesis and cancer progression. BMP9 signals through ALK2 in non-endothelial cells such as in ovarian epithelium, where it has been shown to promote ovarian cancer cell proliferation (8). Similarly, in hepatocellular carcinoma BMP9 has been reported to act as proliferative and survival factor (10). Studies have also highlighted the role of BMP9 in reducing breast cancer cell growth and metastasis (45-47). However, the role of BMP9 and ALKs in promoting or suppressing different cancer types remains controversial. Collectively, this indicates that the effect of BMP9 on tumor promotion vs tumor suppression could be context and cancer-type specific, thus providing the rationale for to elucidate the role of BMP9 in prostate cancer, for which no information is available to our knowledge.

We searched publicly available databases of human prostate cancer specimens and found that ALK2 is significantly upregulated in malignant vs. benign tumor tissue samples whereas ALK1 has the opposite expression pattern, although shown to correlate with poor survival in other dataset (35). However, these data are consistent with our model in which the tumor-promoting effects of BMP9 are mediated by ALK2. Additionally, microarray analysis of data from mouse prostate intraepithelial neoplasia (PIN) versus invasive cancer in a multistage model of prostate carcinogenesis showed up-regulation of ALK2 and BMP9 at the invasive stage in the stromal compartment (48). Taken together, these data suggest a tumor-promoting role of BMP9 produced by the supportive stroma during prostate cancer progression. The fact that the BMP9 transcript levels registered in the selected dataset are similar in benign vs tumor stage in human prostate tumor samples, suggests a paracrine effect of BMP9 in human prostate cancer (35). Moreover, the significant increased expression of ALK2 in human prostate tumor tissue samples suggests that the BMP9 produced by the stromal compartment might be pro-tumorigenic as suggested by the anti-tumor effect of ALK1Fc that we have

documented here. This hypothesis is reinforced by our survival analysis which shows that BMP9 correlates with poor survival in human prostate cancer patients.

Our *in vitro* findings strengthen the afore-mentioned expression data and suggest that BMP9 increases proliferation of human prostate cancer cells. Moreover, our studies incorporating blockade of ALK2 activity by LDN193189 support the notion that ALK2 is critically involved in mediating BMP9-induced proliferation. As depicted in the supplementary data, treatment with ALK1Fc or LDN193189 alone did not affect proliferation of human prostate cancer cells suggesting a paracrine effect of stroma-derived BMP9 on tumor cells. While BMP9 did not influence clonogenic ability of human prostate cancer cells, it elicited a significant stimulatory effect on colony size suggesting it influences colony expansion rather than colony formation.

In our orthotopic model of human prostate cancer, ALK1Fc significantly reduced the prostate tumor burden compared to the control group and vascular density was also reduced in animals treated with ALK1Fc versus those treated with CFc. Interestingly, lectin distribution appeared to be less diffuse in ALK1Fc treated animals, suggesting an effect on vessel maintenance rather than angiogenesis. Strikingly, ALK1Fc treatment of tumor-bearing animals resulted in highly hypoxic tumors with a decreased number of CD31+ tumor capillaries suggesting that ALK1Fc may block BMP9-induced neovascularization.

As expected, areas of tumor proliferation and apoptosis were found to be mutually exclusive in their distribution. Apoptotic regions overlapped with hypoxic areas, suggesting that blockade of BMP9 by ALK1Fc might have an effect on proliferation and apoptosis of human prostate cancer cells in addition to targeting vessel maintenance (28).

SMAD1 and SMAD5 are intracellular effectors of BMP9 signaling that can directly interact with the JAG1 promoter following BMP9 treatment (49) and induce transcription of the NOTCH ligand JAG1 (41). Transcriptional analysis revealed that ALK1Fc systemically blocks the induction of JAG1 mRNA in the presence of BMP9 (49) supporting our hypothesis that the crosstalk between BMP9 and NOTCH signaling may have clinical implications in prostate cancer. Indeed, *in silico* analysis of a previously published dataset of human prostate cancer specimens confirms that both *NOTCH1* and *JAG1* are upregulated at the tumor stage (35). Our database analysis in a multistage model of prostate carcinogenesis on mouse prostate intraepithelial neoplasia (PIN) vs. invasive cancer further indicates that *Jag1* is significantly upregulated in the stroma during the invasive cancer stage (48).

Interestingly, NOTCH activates aldehyde dehydrogenase 1A1 (ALDH1A1) a well-known marker of highly tumorigenic prostate cancer stem-like cells (23-25). The $ALDH^{high}$ subpopulation contributes to both tumor initiation and progression and when highly

expressed in advanced-stage cancers correlates with poor survival in hormone-naïve patients (25). ALK1Fc-treated tumors showed significant reduction of ALDH1A1, which in combination with the data described above, suggests that ALK1Fc might potentially interfere with NOTCH signaling in the regulation of ALDH1A1.
In conclusion, our findings provide novel information on the role of BMP9 in human prostate cancer and suggest the promising use of BMP9 targeting molecules for the treatment of tumor and supportive microenvironment in prostate cancer patients.

Acknowledgements

We thank Acceleron Pharma for providing the ALK1Fc (RAP-041), Laurens van Meeteren and Marjan van de Merbel. The research leading to these results has received funding from the FP7 Marie Curie ITN under grant agreement No. 264817 - BONE-NET (EZ) and from the Netherlands Initiative of Regenerative Medicine (NIRM, grant No. FES0908).

REFERENCES

1. Jemal A, Center MM, DeSantis C and Ward EM. Global patterns of cancer incidence and mortality rates and trends. Cancer Epidemiol Biomarkers Prev. 2010; 19(8):1893-1907.
2. Ye L, Lewis-Russell JM, Kyanaston HG and Jiang WG. Bone morphogenetic proteins and their receptor signaling in prostate cancer. Histol Histopathol. 2007; 22(10):1129-1147.
3. Bendell JC, Gordon MS, Hurwitz HI, Jones SF, Mendelson DS, Blobe GC, Agarwal N, Condon CH, Wilson D, Pearsall AE, Yang Y, McClure T, Attie KM, Sherman ML and Sharma S. Safety, pharmacokinetics, pharmacodynamics, and antitumor activity of dalantercept, an activin receptor-like kinase-1 ligand trap, in patients with advanced cancer. Clinical cancer research : an official journal of the American Association for Cancer Research. 2014; 20(2):480-489.
4. Hawinkels LJ, Garcia de Vinuesa A and Ten Dijke P. Activin receptor-like kinase 1 as a target for anti-angiogenesis therapy. Expert Opin Investig Drugs. 2013; 22(11):1371-1383.
5. van Meeteren LA, Thorikay M, Bergqvist S, Pardali E, Gallo Stampino C, Hu-Lowe D, Goumans M-J and ten Dijke P. Anti-human Activin receptor-like kinase 1 (ALK1) antibody attenuates Bone morphogenetic protein 9 (BMP9)-induced ALK1 signaling and interferes with endothelial cell sprouting. Journal of Biological Chemistry. 2012; 287(22):18551-18561.
6. Bragdon B, Moseychuk O, Saldanha S, King D, Julian J and Nohe A. Bone morphogenetic proteins: a critical review. Cellular Signaling. 2011; 23(4):609-620.
7. David L, Mallet C, Mazerbourg S, Feige JJ and Bailly S. Identification of BMP9 and BMP10 as functional activators of the orphan activin receptor-like kinase 1 (ALK1) in endothelial cells. Blood. 2007; 109(5):1953-1961.
8. Herrera B, van Dinther M, Ten Dijke P and Inman GJ. Autocrine bone morphogenetic protein-9 signals through activin receptor-like kinase-2/Smad1/Smad4 to promote ovarian cancer cell proliferation. Cancer research. 2009; 69(24):9254-9262.
9. Scharpfenecker M, van Dinther M, Liu Z, van Bezooijen RL, Zhao Q, Pukac L, Lowik CW and ten Dijke P. BMP-9 signals via ALK1 and inhibits bFGF-induced endothelial cell proliferation and VEGF-stimulated angiogenesis. J Cell Sci. 2007; 120(Pt 6):964-972.
10. Herrera B, Garcia-Alvaro M, Cruz S, Walsh P, Fernandez M, Roncero C, Fabregat I, Sanchez A and Inman GJ. BMP9 is a proliferative and survival factor for human hepatocellular carcinoma cells. PloS one. 2013; 8(7):e69535.
11. Li R, Zhang W, Cui J, Shui W, Yin L, Wang Y, Zhang H, Wang N, Wu N, Nan G, Chen X, Wen S, Deng F, Zhang H, Zhou G, Liao Z, et al. Targeting BMP9-promoted human osteosarcoma growth by inactivation of notch signaling. Current cancer drug targets. 2014; 14(3):274-285.
12. Celeste AJ SJ, Cox K, Rosen V, Wozney JM. Bone morphogenetic protein-9, a new member of the TGF-beta superfamily. J Bone Min Res. 1994; Supp 1(136).
13. Wang K, Feng H, Ren W, Sun X, Luo J, Tang M, Zhou L, Weng Y, He T-C and Zhang Y. BMP9 inhibits the proliferation and invasiveness of breast cancer cells MDA-MB-231. Journal of cancer research and clinical oncology. 2011; 137(11):1687-1696.
14. Ye L, Kynaston H and Jiang WG. Bone morphogenetic protein-9 induces apoptosis in prostate cancer cells, the role of prostate apoptosis response-4. Molecular Cancer Research. 2008; 6(10):1594-1606.
15. Olsen OE, Wader KF, Misund K, Vatsveen TK, Ro TB, Mylin AK, Turesson I, Stordal BF, Moen SH, Standal T, Waage A, Sundan A and Holien T. Bone morphogenetic protein-9 suppresses

growth of myeloma cells by signaling through ALK2 but is inhibited by endoglin. Blood Cancer Journal. 2014; 4:e196.

16. Cunha SI and Pietras K. ALK1 as an emerging target for antiangiogenic therapy of cancer. Blood. 2011; 117(26):6999-7006.
17. Urness LD, Sorensen LK and Li DY. Arteriovenous malformations in mice lacking activin receptor-like kinase-1. Nature genetics. 2000; 26(3):328-331.
18. Gale NW, Dominguez MG, Noguera I, Pan L, Hughes V, Valenzuela DM, Murphy AJ, Adams NC, Lin HC, Holash J, Thurston G and Yancopoulos GD. Haploinsufficiency of delta-like 4 ligand results in embryonic lethality due to major defects in arterial and vascular development. Proceedings of the National Academy of Sciences of the United States of America. 2004; 101(45):15949-15954.
19. Krebs LT, Shutter JR, Tanigaki K, Honjo T, Stark KL and Gridley T. Haploinsufficient lethality and formation of arteriovenous malformations in Notch pathway mutants. Genes & development. 2004; 18(20):2469-2473.
20. Carvalho FL, Simons BW, Eberhart CG and Berman DM. Notch signaling in prostate cancer: a moving target. The Prostate. 2014; 74(9):933-945.
21. Ross AE, Marchionni L, Vuica-Ross M, Cheadle C, Fan J, Berman DM and Schaeffer EM. Gene expression pathways of high grade localized prostate cancer. The Prostate. 2011.
22. Wang Z, Li Y, Banerjee S, Kong D, Ahmad A, Nogueira V, Hay N and Sarkar FH. Down-regulation of Notch-1 and Jagged-1 inhibits prostate cancer cell growth, migration and invasion, and induces apoptosis via inactivation of Akt, mTOR, and NF-kappaB signaling pathways. J Cell Biochem. 2010; 109(4):726-736.
23. Zhao D, Mo Y, Li M-T, Zou S-W, Cheng Z-L, Sun Y-P, Xiong Y, Guan K-L and Lei Q-Y. NOTCH-induced aldehyde dehydrogenase 1A1 deacetylation promotes breast cancer stem cells. The Journal of Clinical Investigation. 2014; 124(12):0-0.
24. Ginestier C, Hur MH, Charafe-Jauffret E, Monville F, Dutcher J, Brown M, Jacquemier J, Viens P, Kleer CG, Liu S, Schott A, Hayes D, Birnbaum D, Wicha MS and Dontu G. ALDH1 is a marker of normal and malignant human mammary stem cells and a predictor of poor clinical outcome. Cell stem cell. 2007; 1(5):555-567.
25. Le Magnen C, Bubendorf L, Rentsch CA, Mengus C, Gsponer J, Zellweger T, Rieken M, Thalmann GN, Cecchini MG, Germann M, Bachmann A, Wyler S, Heberer M and Spagnoli GC. Characterization and clinical relevance of ALDHbright populations in prostate cancer. Clinical cancer research : an official journal of the American Association for Cancer Research. 2013; 19(19):5361-5371.
26. Li T, Su Y, Mei Y, Leng Q, Leng B, Liu Z, Stass SA and Jiang F. ALDH1A1 is a marker for malignant prostate stem cells and predictor of prostate cancer patients' outcome. Laboratory investigation; a journal of technical methods and pathology. 2010; 90(2):234-244.
27. Seehra J, Knopf J, Pearsall RS, Grinberg A and Kumar R. (2009). Antagonists of bmp9, bmp10, alk1 and other alk1 ligands, and uses thereof. Google Patents).
28. Mitchell D, Pobre EG, Mulivor AW, Grinberg AV, Castonguay R, Monnell TE, Solban N, Ucran JA, Pearsall RS, Underwood KW, Seehra J and Kumar R. ALK1-Fc inhibits multiple mediators of angiogenesis and suppresses tumor growth. Mol Cancer Ther. 2010; 9(2):379-388.
29. Cunha SI, Pardali E, Thorikay M, Anderberg C, Hawinkels L, Goumans M-J, Seehra J, Heldin C-H, ten Dijke P and Pietras K. Genetic and pharmacological targeting of activin receptor-like

kinase 1 impairs tumor growth and angiogenesis. The Journal of Experimental Medicine. 2010; 207(1):85-100.

30. Suzuki Y, Ohga N, Morishita Y, Hida K, Miyazono K and Watabe T. BMP-9 induces proliferation of multiple types of endothelial cells in vitro and in vivo. Journal of Cell Science. 2010; 123(10):1684-1692.
31. Kroon J, In 't Veld LS, Buijs JT, Cheung H, van der Horst G and van der Pluijm G. Glycogen synthase kinase-3beta inhibition depletes the population of prostate cancer stem/progenitor-like cells and attenuates metastatic growth. Oncotarget. 2014; 5(19):8986-8994.
32. Craft CS, Romero D, Vary CP and Bergan RC. Endoglin inhibits prostate cancer motility via activation of the ALK2-Smad1 pathway. Oncogene. 2007; 26(51):7240-7250.
33. Shi S, Hoogaars WM, de Gorter DJ, van Heiningen SH, Lin HY, Hong CC, Kemaladewi DU, Aartsma-Rus A, ten Dijke P and t Hoen PA. BMP antagonists enhance myogenic differentiation and ameliorate the dystrophic phenotype in a DMD mouse model. Neurobiology of disease. 2011; 41(2):353-360.
34. Cuny GD, Yu PB, Laha JK, Xing X, Liu JF, Lai CS, Deng DY, Sachidanandan C, Bloch KD and Peterson RT. Structure-activity relationship study of bone morphogenetic protein (BMP) signaling inhibitors. Bioorganic & medicinal chemistry letters. 2008; 18(15):4388-4392.
35. Borno ST, Fischer A, Kerick M, Falth M, Laible M, Brase JC, Kuner R, Dahl A, Grimm C, Sayanjali B, Isau M, Rohr C, Wunderlich A, Timmermann B, Claus R, Plass C, et al. Genome-wide DNA methylation events in TMPRSS2-ERG fusion-negative prostate cancers implicate an EZH2-dependent mechanism with miR-26a hypermethylation. Cancer discovery. 2012; 2(11):1024-1035.
36. Bacac M, Provero P, Mayran N, Stehle J-C, Fusco C and Stamenkovic I. A mouse stromal response to tumor invasion predicts prostate and breast cancer patient survival. PloS one. 2006; 1(1):e32.
37. Shou J, Ross S, Koeppen H, de Sauvage FJ and Gao WQ. Dynamics of notch expression during murine prostate development and tumorigenesis. Cancer research. 2001; 61(19):7291-7297.
38. Zhang Y, Wang Z, Ahmed F, Banerjee S, Li Y and Sarkar FH. Down-regulation of Jagged-1 induces cell growth inhibition and S phase arrest in prostate cancer cells. International journal of cancer Journal international du cancer. 2006; 119(9):2071-2077.
39. Leong KG and Gao WQ. The Notch pathway in prostate development and cancer. Differentiation. 2008; 76(6):699-716.
40. Bin Hafeez B, Adhami VM, Asim M, Siddiqui IA, Bhat KM, Zhong W, Saleem M, Din M, Setaluri V and Mukhtar H. Targeted knockdown of Notch1 inhibits invasion of human prostate cancer cells concomitant with inhibition of matrix metalloproteinase-9 and urokinase plasminogen activator. Clinical cancer research : an official journal of the American Association for Cancer Research. 2009; 15(2):452-459.
41. Larrivee B, Prahst C, Gordon E, del Toro R, Mathivet T, Duarte A, Simons M and Eichmann A. ALK1 signaling inhibits angiogenesis by cooperating with the Notch pathway. Dev Cell. 2012; 22(3):489-500.
42. David L, Mallet C, Mazerbourg S, Feige J-J and Bailly S. (2007). Identification of BMP9 and BMP10 as functional activators of the orphan activin receptor-like kinase 1 (ALK1) in endothelial cells.
43. Siegel PM and Massague J. Cytostatic and apoptotic actions of TGFβ in homeostasis and cancer. Nat Rev Cancer. 2003; 3(11):807-820.

44. Massagué J. TGFβ in Cancer. Cell. 2008; 134(2):215-230.
45. Wang K, Feng H, Ren W, Sun X, Luo J, Tang M, Zhou L, Weng Y, He TC and Zhang Y. BMP9 inhibits the proliferation and invasiveness of breast cancer cells MDA-MB-231. Journal of cancer research and clinical oncology. 2011; 137(11):1687-1696.
46. Ren W, Sun X, Wang K, Feng H, Liu Y, Fei C, Wan S, Wang W, Luo J, Shi Q, Tang M, Zuo G, Weng Y, He T and Zhang Y. BMP9 inhibits the bone metastasis of breast cancer cells by downregulating CCN2 (connective tissue growth factor, CTGF) expression. Molecular biology reports. 2014; 41(3):1373-1383.
47. Ren W, Liu Y, Wan S, Fei C, Wang W, Chen Y, Zhang Z, Wang T, Wang J, Zhou L, Weng Y, He T and Zhang Y. BMP9 inhibits proliferation and metastasis of HER2-positive SK-BR-3 breast cancer cells through ERK1/2 and PI3K/AKT pathways. PloS one. 2014; 9(5):e96816.
48. Bacac M, Provero P, Mayran N, Stehle JC, Fusco C and Stamenkovic I. A mouse stromal response to tumor invasion predicts prostate and breast cancer patient survival. PloS one. 2006; 1:e32.
49. Morikawa M, Koinuma D, Tsutsumi S, Vasilaki E, Kanki Y, Heldin CH, Aburatani H and Miyazono K. ChIP-seq reveals cell type-specific binding patterns of BMP-specific Smads and a novel binding motif. Nucleic acids research. 2011; 39(20):8712-8727.
50. Berridge MV, Herst PM and Tan AS. (2005). Tetrazolium dyes as tools in cell biology: new insights into their cellular reduction. Biotechnology Annual Review: Elsevier), pp. 127-152.
51. van der Pluijm G, Que I, Sijmons B, Buijs JT, Lowik CW, Wetterwald A, Thalmann GN, Papapoulos SE and Cecchini MG. Interference with the microenvironmental support impairs the de novo formation of bone metastases in vivo. Cancer Res. 2005; 65(17):7682-7690.
52. Karkampouna S, Kruithof BP, Kloen P, Obdeijn MC, van der Laan AM, Tanke HJ, Kemaladewi DU, Hoogaars WM, t Hoen PA, Aartsma-Rus A, Clark IM, Ten Dijke P, Goumans MJ and Kruithof-de Julio M. Novel ex vivo culture method for the study of Dupuytren's Disease: effects of TGFβ type 1 receptor modulation by antisense oligonucleotides. Molecular therapy Nucleic acids. 2014; 3:e142.
53. Guzman C, Bagga M, Kaur A, Westermarck J and Abankwa D. ColonyArea: an ImageJ plugin to automatically quantify colony formation in clonogenic assays. PLoS One. 2014; 9(3):e92444.

SUPPLEMENTARY DATA

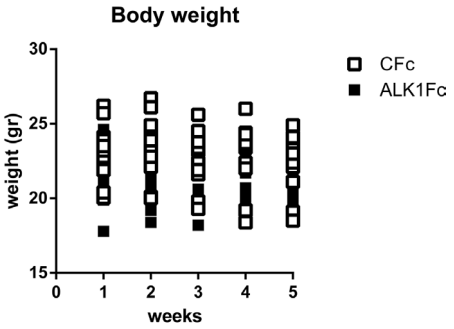

Suppl. Fig. 1 Body weight of animals used for *in vivo* experiment. Body weight (grams) of all the animals of treatment groups measured weekly during the course of treatment with either CFc (n=6) or ALK1Fc (n=7).

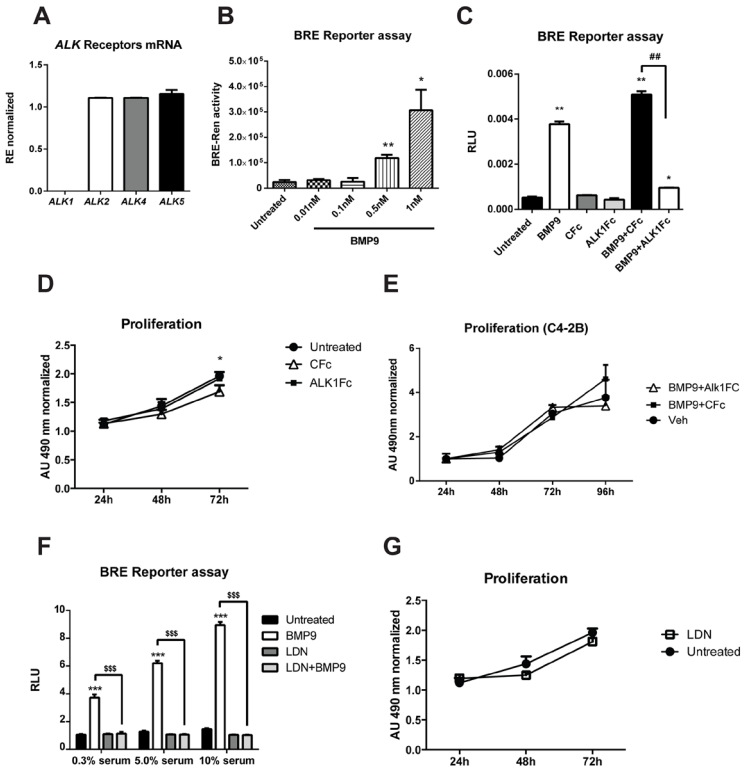

Suppl. Fig. 2 Characterization of dose response for BMP9 with luciferase reporter. **A**) Endogenous expression of *ALK1*, *ALK2*, *ALK4* and *ALK5* receptors in PC-3M-Pro4Luc2cells (mRNA level). Relative expression levels normalized to β-actin are shown. Error bars indicate +/-SD. **B**) Dose dependent response of PC-3M-Pro4Luc2 cells to recombinant BMP9 (0.01, 0.1, 0.5, 1 nM). Downstream activation of BMP signaling was tested by transfection of BRE-renilla construct and measured by reporter activity assay. Graph represents values from three independent experiments; error bars indicate ± SEM (n=3). P value < 0.05 (*) and P value < 0.01 (**). **C**) BRE reporter luciferase (BREluc) assay; Inhibitory concentration of ALK1Fc or CFc (10 ug/ml) was determined in cells stimulated with 1 nM BMP9. Graph represents values from two independent experiments; error bars indicate ± SEM (n=2). P value < 0.05 (*) and P value < 0.01 (**) compared to "untreated" control. P value < 0.01 (##) **D**) MTS assay (24, 48, 72 hours) was performed in PC-3M-Pro4-luc2 human prostate cancer cell line treated with recombinant ALK1Fc (10 ug/ml), CFc (10 ug/ml). Accumulation of MTS was measured based on absorbance at 490 nm. Values are normalized to the basal measurements at 24 hours after cell seeding and treatments. Graph represents values from two independent experiments (n=2). Error bars indicate ±SEM. **E**) MTS assay (24, 48, 72, 96 hours) was performed in C4-2B human prostate cancer cell lines stimulated with recombinant BMP9 (1 nM), BMP9 (1 nM)+ALK1Fc (10 ug/ml) or BMP9 (1 nM)+CFc (10 ug/ml). (n=3). **F**) BMP promoter assay (BRE-luciferase). PC-3M-Pro4 were seeded and, transfected with BRE-luc and renilla plasmid DNA. After 24 hours the medium was replaced with 0.3%, 5%, 10% FCII serum containing media and treated with BMP9 (1nM), LDN193189 (LDN, 120nM) and BMP9+LDN. Luc and Ren values were measured 24 hrs after treatment. RLU ratio values are shown (Luc/Ren). Error bars indicate ±SD. **G**) MTS assay (24, 48, 72

hours) was performed in PC-3M-Pro4-luc2 human prostate cancer cell line treated with LDN inhibitor (LDN193189, 120 nM). (n=2). Error bars indicate +/-SEM.

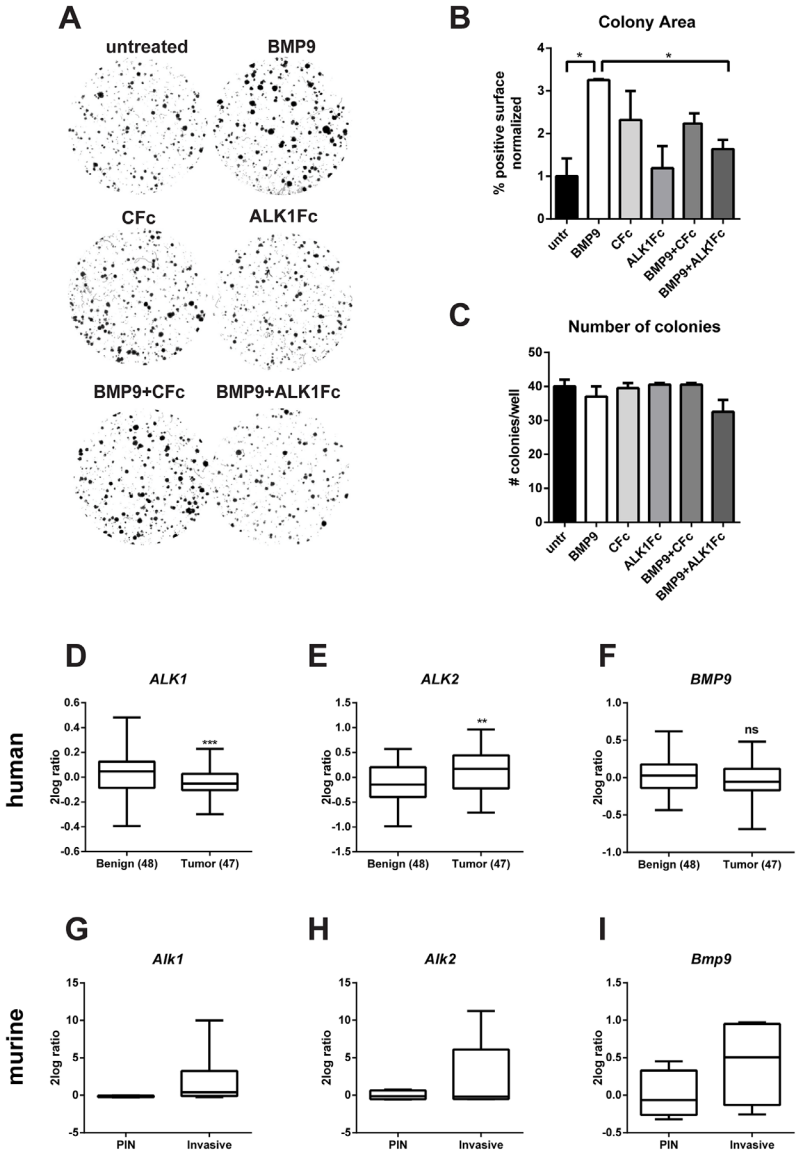

Suppl. Fig. 3 Effect of BMP9 and ALK1Fc on clonogenicity and ALK expression in human samples. A) Clonogenic assay of PC-3M-Pro4Luc2 cells. Low-density cultures (100 cells per well of 6well plate) were stimulated with BMP9, CFc, ALK1Fc, BMP9+CFc, BMP9+ALK1Fc. Colony formation was assessed after 10 days by crystal violet staining. Representative images are shown. **B-C**) Quantification of surface covered by crystal violet positive colonies (colony area) and colony number. Graph shows percentage of positive

surface normalized per condition (average of three independent experiments). P value < 0.05 (*). Error bars indicate SEM. **D-F**) Bioinformatics analysis of AMC OncoGenomics database (Sueltman transcript comparison) showing mRNA expression of *ALK1, ALK2* and *BMP9* in prostate tissues among benign prostate tissues (n=48) versus tumor tissues (n=47). Values are expressed as 2log ratio tumor/ benign. ns: non-significant. P value < 0.01 (**) **G-I**) Microarray cDNA analysis (adapted from *Bacac et al.,* (36) of *Alk1, Alk2* and *Bmp9* expression in microdissected murine stroma derived from two tumor stages; prostate intraepithelial neoplasia (PIN, n=4), and invasive tumors (n=6).

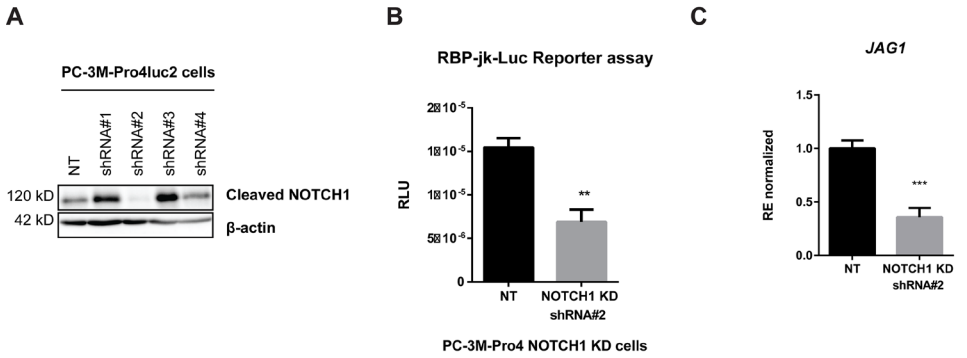

Suppl.Fig.4. Characterization of NOTCH1 knock-down. **A**) Western immunoblotting for NOTCH1 protein as validation of lentiviral shRNA-mediated knockdown of NOTCH1 intracellular domain (cleaved) in PC-3M-Pro4luc2 PCa cell line using five shRNA constrcuts. Based on the downregulation of cleaved NOTCH1 observed after lentiviral transduction and puromycin selection, the stable line expressing the shRNA #2 construct was selected for further experiments. NT; non-targeting shRNA lentiviral mediated transduction. B-actin was used as loading control. **B**) NOTCH transcription factor RBP-Jk-luciferase reporter assay in non-targeting (NT) and NOTCH1 (shRNA#2) knockdown (KD) PC-3M-Pro4Luc2 cells. RLU: relative luciferase units (signal of luciferase normalised to renilla values). n=3, P value < 0.01 (**) **C**) QPCR for *JAG1* mRNA levels in non-targeting (NT) and NOTCH1 (shRNA#2) knockdown (KD) PC-3M-Pro4Luc2 cells. Fold over the value of NT is represented. Error bars indicate ±SD. P value < 0.001 (***).